Acta Mech 228, 415–431 (2017)
DOI 10.1007/s00707-016-1710-6

ORIGINAL PAPER

Qing Chen · Zhengwu Jiang · Zhenghong Yang · Hehua Zhu · J. Woody Ju · Zhiguo Yan · Yaqiong Wang

Differential-scheme based micromechanical framework for unsaturated concrete repaired by the electrochemical deposition method

Received: 24 April 2016 / Revised: 2 August 2016 / Published online: 26 September 2016

Abstract Most concrete structures repaired by the electrochemical deposition method (EDM) are not fully saturated in reality. Based on our latest work, a differential-scheme-based micromechanical framework is presented to predict the properties of unsaturated concrete repaired by the EDM. The equivalent matrix is reached by the micromechanical homogenization to the two-phase composite composed by the intrinsic concrete and unsaturated pores with different shapes. According to the multiphase micromechanical healing model which we presented recently, the three different states of the healing process in the saturated zone of the unsaturated concrete, including no healing, partial healing and complete healing, are quantitatively investigated by modifying the differential-scheme and the generalized self-consistent method with the obtained equivalent matrix. Modification procedures are utilized to rationalize the differential-scheme-based estimations for the repaired concrete in the dry state. Furthermore, predictions herein are compared with those of the existing models and available experimental results, thus illustrating the feasibility and capability of the proposed micromechanical framework. It is found that the predictions in this extension correspond to the experimental data better than those of our recent work.

1 Introduction

As a promising approach to repair concrete cracks, the electrochemical deposition method (EDM) has been applied to marine structures or other situations in which traditional repairing methods are not adequate [1–3]. Extensive works have been conducted on the EDM in the past 20 years [4–14]. However, existing literature mainly focuses on the experimental procedures, and few studies have disclosed the healing mechanism of

Q. Chen · Z. Jiang (✉) · Z. Yang
Key Laboratory of Advanced Civil Engineering Materials of Ministry of Education, Tongji University, 4800 Cao'an Road, Shanghai 201804, China
E-mail: m2ludear@126.com

Q. Chen · Y. Wang
Shaanxi Provincial Major Laboratory for Highway Bridge and Tunnel, Chang'an University, Xi'an 710064, Shaanxi, China

H. Zhu · Z. Yan
State Key Laboratory for Disaster Reduction in Civil Engineering, Tongji University, 1239 Siping Road, Shanghai 200092, China

H. Zhu · Z. Yan
Key Laboratory of Geotechnical and Underground Engineering of the Ministry of Education, Tongji University, 1239 Siping Road, Shanghai 200092, China

J. W. Ju
Department of Civil and Environmental Engineering, University of California, Los Angeles, CA 90095, USA

the EDM with rigorous analytical models, particularly the micromechanical models at the microstructural level. To address these issues, the authors recently proposed micromechanical models for saturated concrete based on the Mori–Tanaka method [15], where the repaired saturated concrete was represented by three-phase composite consisting of the intrinsic concrete (including the mortar, coarse aggregates and their interfaces), deposition product and water phase. The Mori–Tanaka method was adopted to derive the effective properties of the repaired concrete.

However, many experimental investigations show that concrete in aqueous environments is not fully saturated even when it is stored in water for a long time [16–20]. As it is very hard for the external solution to reach the dry or unsaturated zone of the concrete samples, those places cannot be healed using the EDM [21]. Since this situation is very different from that occurring in fully saturated concrete, the authors recently presented a multiphase micromechanical model for unsaturated concrete repaired by the EDM based on the Mori–Tanaka method to describe this distinct phenomenon [21]. The accuracy of the Mori–Tanaka method is high when the volume fraction of the inclusion is low [21]. However, with an increase in the inclusion volume fractions, the Mori–Tanaka method may underestimate (or overestimate) the effective properties of the composite when the properties of the inclusion phase are stronger (or weaker) than those of the matrix phase [21]. As an extension of Yan et al. [21], an equivalent matrix for unsaturated concrete is attained through the micromechanical homogenization to a two-phase composite composed by the intrinsic concrete and unsaturated pores with different shapes. Meanwhile, with the obtained equivalent matrix, a differential-scheme-based micromechanical framework is proposed in this work to quantitatively characterize and predict the mechanical performance of unsaturated concrete healed by the EDM. Three different states of the healing process, including no healing, partial healing and complete healing, are quantitatively investigated by incorporating the differential-scheme and the generalized self-consistent method together based on the multiphase healing model we presented recently. Furthermore, micromechanical procedures are adopted to modify the properties of the healed concrete in the dry state.

An outline of this paper is organized as follows. Section 2 introduces the micromechanical model for the unsaturated concrete repaired by the EDM. The equivalent matrix is obtained by the homogenization to the two-phase composite consisting of the intrinsic concrete and unsaturated pores with different shapes. In sect. 3, the effective properties at three different states of the healing process are quantitatively predicted by modifying the differential scheme for unsaturated concrete repaired by the EDM. Furthermore, modification procedures are adopted to consider the water effects and shapes of the pores in the healed concrete. Numerical examples including experimental validations and comparisons with existing micromechanical models are presented in Sect. 4. Some conclusions are reached in the final section.

2 Micromechanical model and equivalent matrix for unsaturated concrete repaired by the EDM

2.1 Micromechanical model for unsaturated concrete repaired by the EDM

From the microlevel, the unsaturated concrete repaired by the EDM is composed of the deposition products, pores, water, mortar, coarse aggregates and their interfaces [21,22]. According to the previous works [15,21,23,24], a micromechanical model for the unsaturated concrete element healed by the EDM can be proposed with some proper assumptions, which is exhibited in Fig. 1a. The three traditional solid phases (i.e., mortar, coarse aggregates and their interfaces) are merged into one matrix phase, namely the intrinsic concrete, in a representative volume element (RVE). The deposition products, water and pores in the unsaturated zone are considered as different inclusion phases in the RVE. The shapes of the microcracks and microvoids (occupied by water) in the saturated zones are presumed to be spherical. However, the shapes of these defects in the unsaturated/dry areas are elliptical. The volume of the deposition product is assumed to be proportional to that of each spherical pore in the saturated zone [15,21,23,24].

During the healing process, the water phase in the saturated zone is replaced by the deposition products. By predicting the effective properties using our micromechanical model, the mechanical performance of the unsaturated concrete can be quantitatively assessed during the healing process. In this study, through the micromechanical homogenization, the equivalent matrix composed by the intrinsic concrete and unsaturated pores is obtained. The properties of repaired concrete at different healing states are calculated by incorporating the differential scheme and the generalized self-consistent method.

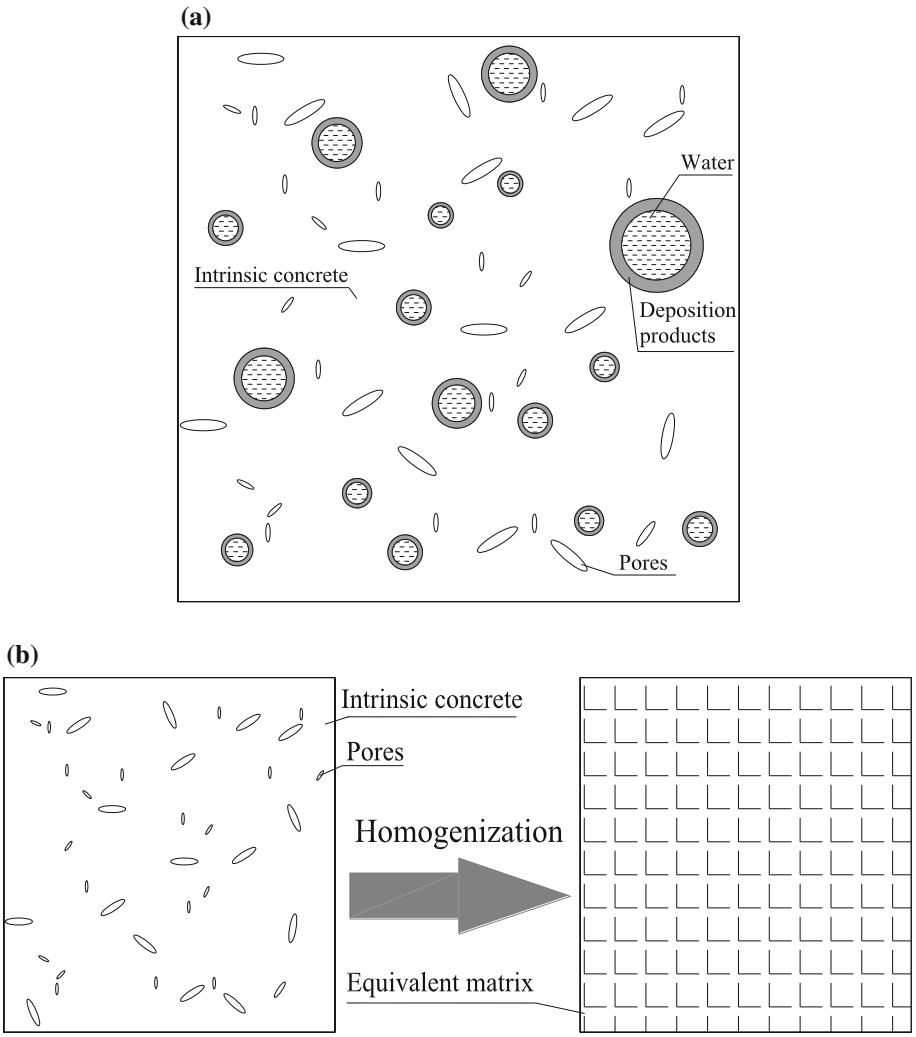

Fig. 1 The micromechanical model and equivalent matrix for unsaturated concrete healed using the EDM. **a** The micromechanical model for unsaturated concrete healed using the EDM. **b** The equivalent matrix for unsaturated concrete healed using the EDM

2.2 The equivalent matrix of the unsaturated concrete repaired by EDM

As exhibited in Fig. 1b, the equivalent matrix of the unsaturated concrete repaired by the EDM can be obtained by micromechanical homogenization to the two-phase composite composed by the intrinsic concrete and the unsaturated pores. According to [25], by replacing its matrix phase with the intrinsic concrete, the properties of the equivalent matrix can be calculated by the iterative scheme below:

$$(K^*)_{n+1} = \frac{(1-\phi_{\mathrm{up}})K_{\mathrm{ic}}(P^{*2})_n}{(\phi_{\mathrm{up}})(P^{*1})_n + (1-\phi_{\mathrm{up}})(P^{*2})_n}, \tag{1}$$

$$(\mu^*)_{n+1} = \frac{(1-\phi_{\mathrm{up}})\mu_{\mathrm{ic}}(Q^{*2})_n}{(\phi_{\mathrm{up}})(Q^{*1})_n + (1-\phi_{\mathrm{up}})(Q^{*2})_n}, \tag{2}$$

$$\phi_{\mathrm{up}} = \frac{(1-S_{\mathrm{eff}})\phi_{\mathrm{eff}}}{(1-S_{\mathrm{eff}})\phi_{\mathrm{eff}} + 1 - \phi_{\mathrm{eff}}}, \tag{3}$$

with

$$\phi_{\text{eff}} = m(k_{\text{p}}, t, v)\phi, \tag{4}$$

$$S_{\text{eff}} = \frac{V_{P-sat}}{V_{\text{P}}} = h(k_{\text{p}}, t)S_w, \tag{5}$$

where $(K^*)_{n+1}$, $(\mu^*)_{n+1}$and $(K^*)_n$, $(\mu^*)_n$ are, respectively, the $(n+1)$th and nth approximations of K^* and μ^*, with the first approximations$(K^*)_1 = K_{\text{ic}}$, $(\mu^*)_1 = \mu_{\text{ic}}$. Here, ϕ_{up} is the volume fraction of pores that cannot be healed in the equivalent matrix. K_{ic} and μ_{ic} are the bulk modulus and shear modulus of the intrinsic concrete, respectively. Moreover, $(P^{*1})_n$, $(P^{*2})_n$, $(Q^{*1})_n$ and $(Q^{*2})_n$ are coefficients defined by the nth approximations to K^* and μ^*, i.e., $(K^*)_n$ and $(\mu^*)_n$. In addition, ϕ_{eff} is the effective porosity of unsaturated concrete considering the further hydration effect which decreases the porosity of unsaturated concrete; m is a function of seepage rate (k_{p}), seepage time (t) and the effective viscosity of water (v), and $m < 1$ for wet concrete; ϕ is the porosity of dry concrete [21,22]. S_{eff} is the effective saturation degree; $V_{\text{P-sat}}$ is the volume of pores that are fully filled with water (or the volume of water in the saturated zone); V_{P} is the total volume of pores in the concrete (including the pores filled with water, unsaturated pores and dry pores); S_w is the general saturation degree; h is a function of seepage rate (k_{p}) and seepage time (t); and h is less than 1 [21,22].

When the inclusions are shaped as penny cracks, these coefficients are calculated as below [25]:

$$(P^{*1})_n = \frac{(K^*)_n}{\pi\alpha(\beta^*)_n}, \tag{6}$$

$$(P^{*2})_n = \frac{(K^*)_n + \frac{4}{3}\mu_{\text{ic}}}{K_{\text{ic}} + \frac{4}{3}\mu_{\text{ic}} + \pi\alpha(\beta^*)_n}, \tag{7}$$

$$(Q^{*1})_n = \frac{1}{5}\left(1 + \frac{8(\mu^*)_n}{\pi\alpha((\mu^*)_n + 2(\beta^*)_n)} + \frac{4(\mu^*)_n}{3\pi\alpha(\beta^*)_n}\right), \tag{8}$$

$$(Q^{*2})_n = \frac{1}{5}\left(1 + \frac{8(\mu^*)_n}{4\mu_{\text{ic}} + \pi\alpha((\mu^*)_n + 2(\beta^*)_n)} + 2\frac{K_{\text{ic}} + \frac{2}{3}\mu_{\text{ic}} + \frac{2}{3}(\mu^*)_n}{K_{\text{ic}} + \frac{4}{3}\mu_{\text{ic}} + \pi\alpha(\beta^*)_n}\right), \tag{9}$$

with

$$(\beta^*)_n = (\mu^*)_n\frac{(3(K^*)_n + (\mu^*)_n)}{(3(K^*)_n + 4(\mu^*)_n)}, \tag{10}$$

$$\alpha = \frac{1}{N}\sum_{i=1}^{N}\frac{a_i}{b_i}, \tag{11}$$

where α is the equivalent aspect ratio of the pores, a_i and b_i are the lengths of the pores' minor and major axes, respectively, and N is the number of different pores in the unsaturated and dry zones of the concrete. Through this iterative scheme, the $(n+1)$th and nth approximations to K^* and μ^* can be reached. Let K_{em}, μ_{em} be the effective bulk modulus and shear modulus of the equivalent matrix. When the difference of the value between these two successive approximations is sufficiently small (in the present case, this value is 0.0001), the effective properties of the equivalent matrix can be expressed as follows:

$$K_{\text{em}} = (K^*)_n, \tag{12}$$

$$\mu_{\text{em}} = (\mu^*)_n. \tag{13}$$

Furthermore, the Young's modulus and Poisson ratio of the equivalent matrix can be obtained based on the theorem of elasticity, provided that the bulk modulus and shear modulus are known:

$$E_{\text{em}} = \frac{9K_{\text{em}}\mu_{\text{em}}}{3K_{\text{em}} + \mu_{\text{em}}}, \tag{14}$$

$$\nu_{\text{em}} = \frac{3K_{\text{em}} - 2\mu_{\text{em}}}{6K_{\text{em}} + 2\mu_{\text{em}}}, \tag{15}$$

where E_{em} and ν_{em} are the Young's modulus and Poisson ratio of the equivalent matrix.

Based on Eqs. (1)–(15), the quantitative influence of the effective saturation degree and the equivalent aspect ratio can be calculated for the equivalent matrix for given intrinsic matrix properties. Here, the experimental

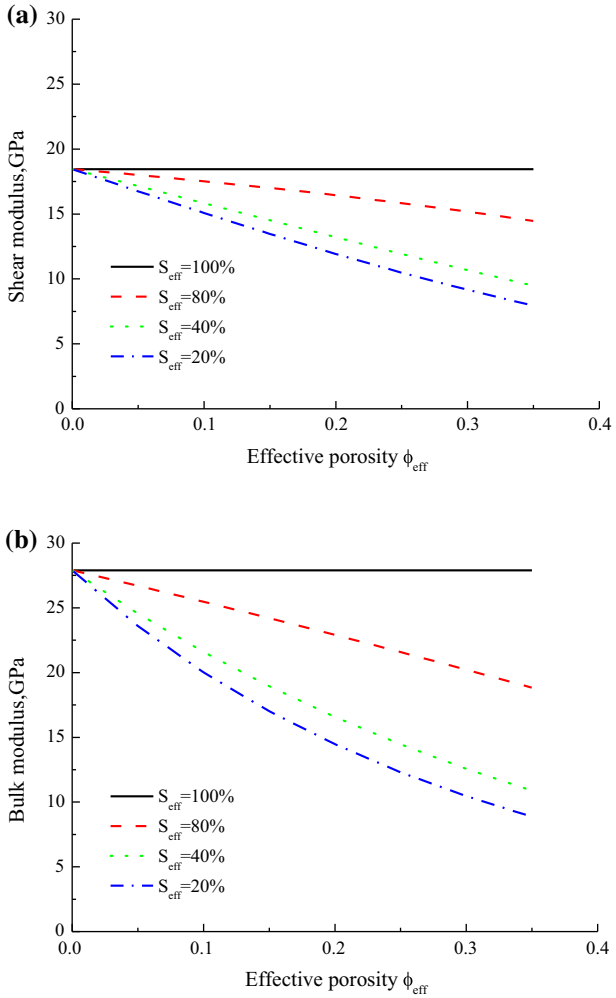

Fig. 2 The effective properties of the equivalent matrix with different effective saturation degrees. **a** The shear modulus, **b** the bulk modulus

data of [26] are employed as the input data in this simulation. The bulk modulus and shear modulus of the intrinsic concrete of [26] are 27.91 and 18.45 GPa, respectively. Figure 2a, b show the effective shear modulus and bulk modulus of the equivalent matrix with different effective saturation degrees. It can be found that the properties of the equivalent matrix decrease with the increase in the porosity. With the increase in the effective saturation degree, the equivalent matrix demonstrates greater properties. As displayed in Fig. 3a, b, the properties of the equivalent matrix decrease with the increase in the effective porosity for a given effective saturation degree. With the increase in the equivalent aspect ratios, the equivalent matrix demonstrates greater properties.

3 Differential-scheme-based micromechanical predictions for effective properties of unsaturated concrete repaired by the EDM

3.1 The differential scheme

In terms of the inclusion-based micromechanical theory and the average stress method [27–32], the effective elastic stiffness tensor of the two-phase composite can be rephrased as

$$\mathbf{D} = \mathbf{D}_0 + \phi\,(\mathbf{D}_I - \mathbf{D}_0)\,\mathbf{A}, \tag{16}$$

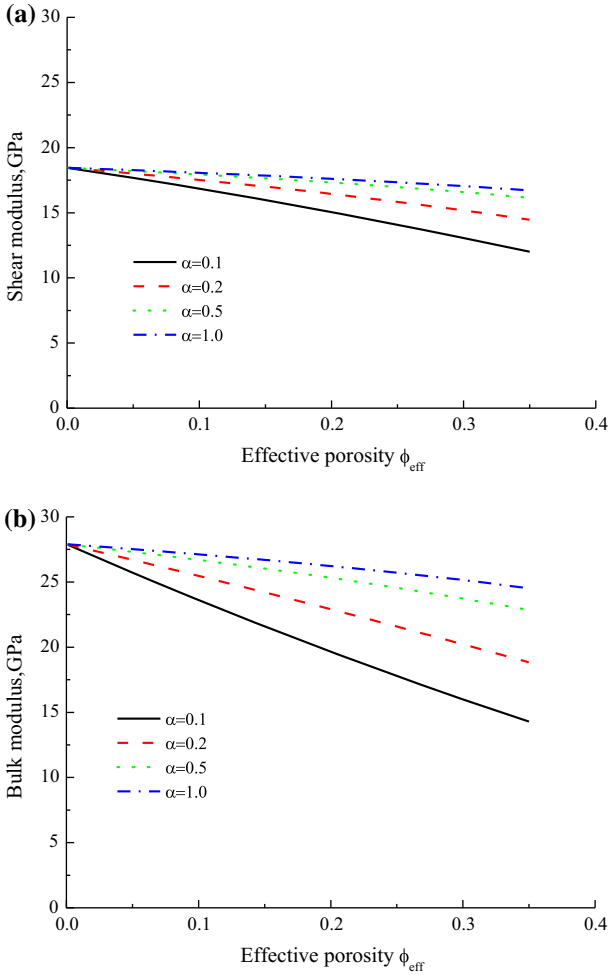

Fig. 3 The effective properties of the equivalent matrix with different equivalent aspect ratios. **a** The shear modulus, **b** the bulk modulus

where $\mathbf{D}_0$ is the elastic stiffness tensor of the matrix phase, $\mathbf{D}_I$ is the elastic stiffness tensor of the inhomogeneity and $\mathbf{A}$ is the strain concentration tensor for the inhomogeneity. Further, ϕ denotes the volume fraction of the inhomogeneity.

Let us define $\phi = \Omega_1/(\Omega_0+\Omega_1)$ and $\phi+\Delta\phi = (\Omega_1+\Delta\Omega)/(\Omega_0+\Omega_1+\Delta\Omega)$, where Ω_0 and $\Omega_1$represent the volume of the matrix phase and the inclusion phase in the current composite, respectively, and $\Delta\Omega$ denotes the increment of inclusion volume. For the differential scheme, a composite with the volume fraction of inclusion equal to $\phi+\Delta\phi$ can be treated as the equivalent composite with the volume fraction of inclusion equal to $\Delta\Omega/(\Omega_0+\Omega_1+\Delta\Omega)$. It is noted that the matrix phase in the equivalent composite is the current composite, which includes the current matrix (Ω_0) and current inclusion (Ω_1). According to Eq. (16), the effective properties of the material can be obtained as [27,28,33,34]

$$\mathbf{D}(\phi+\Delta\phi) = \mathbf{D}(\phi) + \frac{\Delta\Omega}{(\Omega_0+\Omega_1+\Delta\Omega)}(\mathbf{D}_I - \mathbf{D}(\phi))\,\mathbf{A}(\mathbf{D}(\phi)). \tag{17}$$

Equation (17) can be rephrased as below through the simple derivation

$$\frac{\mathbf{D}(\phi+\Delta\phi)-\mathbf{D}(\phi)}{\Delta\phi} = \frac{1}{1-\phi}(\mathbf{D}_I - D(\phi))\,\mathbf{A}(\mathbf{D}(\phi)) \tag{18}$$

with

$$\Delta\phi = \frac{\Omega_1+\Delta\Omega}{\Omega_0+\Omega_1+\Delta\Omega} - \frac{\Omega_1}{\Omega_0+\Omega_1} = \frac{(1-\phi)\Delta\Omega}{(\Omega_0+\Omega_1+\Delta\Omega)}. \tag{19}$$

When $\Delta\phi \to 0$, Eq. (18) can be expressed as

$$\frac{\mathrm{d}\mathbf{D}(\phi)}{d\phi} = \frac{1}{1-\phi} \bullet (\mathbf{D}_I - \mathbf{D}(\phi)) : \mathbf{A}(\mathbf{D}(\phi)). \tag{20}$$

The composite effective properties with no inclusion effects should be the same as those of the matrix phase, which implies

$$\mathbf{D}(\phi)\big|_{\phi=0} = \mathbf{D}_0. \tag{21}$$

When the Eshelby method is considered, we write

$$\mathbf{A} = \left[\mathbf{I} + \mathbf{S}\mathbf{D}(\phi)^{-1}(\mathbf{D}_I - \mathbf{D}(\phi))\right]^{-1}, \tag{22}$$

where S is Eshelby's tensor, which depends on $\mathbf{D}(\phi)$ and the shape of the inclusions, and $\mathbf{I}$ defines the fourth-order isotropic identity tensor.

3.2 The effective properties of unsaturated concrete repaired by the EDM at two extreme states

The first extreme state is that there is no electrochemical deposition product (no healing process) in the concrete at all (which is equal to an unsaturated concrete). Therefore, the only inclusion phase in the equivalent matrix is water itself. Let $\mathbf{D}_w$, $\mathbf{D}_{\mathrm{em}}$ and $\mathbf{D}_{e1}$ represent the stiffness tensor of the water phase, the equivalent matrix and the equivalent composite of the unsaturated concrete predicted by the differential scheme. For the isotropic matrix and spherical equivalent inclusions, the tensorial components of $\mathbf{I}$, $\mathbf{D}_w$, $\mathbf{D}_{\mathrm{em}}$ and $\mathbf{D}_{e1}$ are as follows:

$$I_{ijkl} = \frac{1}{3}\delta_{ij}\delta_{kl} + \frac{1}{2}\left(\delta_{ik}\delta_{jl} + \delta_{il}\delta_{jk} - \frac{2}{3}\delta_{ij}\delta_{kl}\right), \tag{23}$$

$$D_{wijkl} = K_w\delta_{ij}\delta_{kl} + \mu_w\left(\delta_{ik}\delta_{jl} + \delta_{il}\delta_{jk} - \frac{2}{3}\delta_{ij}\delta_{kl}\right), \tag{24}$$

$$D_{\mathrm{em}ijkl} = K_{\mathrm{em}}\delta_{ij}\delta_{kl} + \mu_{\mathrm{em}}\left(\delta_{ik}\delta_{jl} + \delta_{il}\delta_{jk} - \frac{2}{3}\delta_{ij}\delta_{kl}\right), \tag{25}$$

$$D_{e1ijkl} = K_{e1}\delta_{ij}\delta_{kl} + \mu_{e1}\left(\delta_{ik}\delta_{jl} + \delta_{il}\delta_{jk} - \frac{2}{3}\delta_{ij}\delta_{kl}\right), \tag{26}$$

where δ_{ij} is the Kronecker delta, K_w, μ_w are, respectively, the bulk modulus and shear modulus of the water and K_{e1} and μ_{e1} are those of the equivalent composite of the unsaturated concrete predicted by the differential scheme, correspondingly.

By replacing the matrix phase and inhomogeneities (inclusion phase) with the attained equivalent matrix and water, the differential scheme is modified to obtain the effective properties of the unsaturated concrete. By substituting Eqs. (23)–(26) into Eqs. (20)–(22), the effective bulk modulus and shear modulus of the unsaturated concrete are obtained by solving the following nonlinear ordinary differential equations after some derivations:

$$\frac{dK_{e1}}{d\phi_F} + \frac{(K_{e1} - K_w)(3K_{e1} + 4\mu_{e1})}{(1-\phi_F)(3K_w + 4\mu_{e1})} = 0, \tag{27}$$

$$\frac{\mathrm{d}\mu_{e1}}{d\phi_F} + \frac{5\mu_{e1}(\mu_{e1} - \mu_w)(3K_{e1} + 4\mu_{e1})}{(1-\phi_F)[3K_{e1}(3\mu_{e1} + 2\mu_w) + 4\mu_{e1}(2\mu_{e1} + 3\mu_w)]} = 0 \tag{28}$$

$$\phi_F = S_{\mathrm{eff}}\phi_{\mathrm{eff}} \tag{29}$$

with the initial conditions as below:

$$K_{e1}(0) = K_{\mathrm{em}}, \tag{30}$$

$$\mu_{e1}(0) = \mu_{\mathrm{em}}. \tag{31}$$

The second extreme state is that the saturated zone has been completely healed by the EDM. Therefore, the inclusion phase in the equivalent matrix turns to the isotropic spherical deposition products. Suppose that K_{e2} and μ_{e2} (K_{dp} and μ_{dp}) are the bulk modulus and shear modulus of the healed concrete (deposition products). By, respectively, replacing K_{e1}, μ_{e1}, K_w and μ_w in Eqs. (27)–(31) with K_{e2}, μ_{e2}, K_{dp} and μ_{dp}, the effective

properties of healed concrete can be similarly achieved with the differential scheme, which can be expressed as

$$\frac{dK_{e2}}{d\phi_F} + \frac{(K_{e2} - K_{\mathrm{dp}})\,(3K_{e2} + 4\mu_{e2})}{(1-\phi_F)\,(3K_{\mathrm{dp}} + 4\mu_{e2})} = 0, \tag{32}$$

$$\frac{\mathrm{d}\mu_{e2}}{d\phi_F} + \frac{5\mu_{e2}\,(\mu_{e2} - \mu_{\mathrm{dp}})\,(3K_{e2} + 4\mu_{e2})}{(1-\phi_F)\left[3K_{e2}\,(3\mu_{e2} + 2\mu_{\mathrm{dp}}) + 4\mu_{e2}\,(2\mu_{e2} + 3\mu_{\mathrm{dp}})\right]} = 0, \tag{33}$$

with the initial conditions as follows:

$$K_{e2}\,(0) = K_{\mathrm{em}}, \tag{34}$$

$$\mu_{e2}\,(0) = \mu_{\mathrm{em}}. \tag{35}$$

3.3 The effective properties of concreted partially healed by the EDM

As to unsaturated concrete partially healed by the EDM, the two inclusion phases (water and deposition products) in the equivalent matrix should be taken into consideration. According to the previous studies [35–48], the differential-scheme-based two-level homogenization scheme is employed to attain the effective properties of the partially healed concrete, which is a *three-phase* composite made up of the equivalent matrix, the deposition products and the water phase. Through the first-level homogenization, the equivalent inclusion can be obtained with the generalized self-consist model by modifying its inner- and outer-layer phases into the water phase and the deposition products, respectively [49,50]. Accordingly, the effective bulk modulus and shear modulus for the equivalent inclusion can be expressed by Eqs. (36) and (37), correspondingly:

$$K_{\mathrm{ei}} = K_{\mathrm{dp}} + \frac{\phi_{\mathrm{FD}}(K_w - K_{\mathrm{dp}})\,(3K_{\mathrm{dp}} + 4\mu_{\mathrm{dp}})}{3K_{\mathrm{dp}} + 4\mu_{\mathrm{dp}} + 3\,(1-\phi_{\mathrm{FD}})\,(K_w - K_{\mathrm{dp}})}, \tag{36}$$

$$A\left(\frac{\mu_{\mathrm{ei}}}{\mu_{\mathrm{dp}}}\right)^2 + B\left(\frac{\mu_{\mathrm{ei}}}{\mu_{\mathrm{dp}}}\right) + C = 0, \tag{37}$$

where ϕ_{FD} is the volume fraction of the water phase in the two-phase composite composed by the water and the deposition products and K_{dp} andμ_{dp} are the bulk modulus and shear modulus of the deposition product, respectively. Further, K_{ei} and μ_{ei} denote the bulk modulus and the shear modulus for the equivalent inclusion after the first-level homogenization, respectively. A,B and C are parameters dependent on ϕ_{FD}, the properties of the water and those of the deposition products. See details in our previous work [15].

Let us define K_{e3} and μ_{e3} as the effective bulk modulus and shear modulus of the partially healed concrete. In this differential-scheme-based micromechanical framework, these two effective properties can be obtained with the second-level homogenization. Specifically, by, respectively, replacing K_{e1}, μ_{e1}, K_w and μ_w in Eqs. (27)–(31) with K_{e3}, μ_{e3}, K_{ei} and μ_{ei}, the effective properties of the partially healed concrete(K_{e3} and μ_{e3}) can be calculated by solving the following nonlinear ordinary differential equations:

$$\frac{dK_{e3}}{d\phi_F} + \frac{(K_{e3} - K_{\mathrm{ei}})\,(3K_{e3} + 4\mu_{e3})}{(1-\phi_F)\,(3K_{\mathrm{ei}} + 4\mu_{e3})} = 0, \tag{38}$$

$$\frac{\mathrm{d}\mu_{e3}}{d\phi_F} + \frac{5\mu_{e3}\,(\mu_{e3} - \mu_{\mathrm{ei}})\,(3K_{e3} + 4\mu_{e3})}{(1-\phi_F)\,[3K_{e3}\,(3\mu_{e3} + 2\mu_{\mathrm{ei}}) + 4\mu_{e3}\,(2\mu_{e3} + 3\mu_{\mathrm{ei}})]} = 0, \tag{39}$$

with the initial conditions as

$$K_{e3}\,(0) = K_{\mathrm{em}}, \tag{40}$$

$$\mu_{e3}\,(0) = \mu_{\mathrm{em}}. \tag{41}$$

3.4 Modifications to the differential-scheme-based predictions in the dry state

All pores in the saturated zone of the unsaturated concrete are assumed to be spherical in the proposed model. However, this assumption is not reasonable when the specimen is dried; i.e., the pore shape should not be spherical any more. To consider these effects, three modification coefficients, χ_K, χ_μ and χ_E, are similarly employed in the extension:

$$\chi_K = \frac{K_\alpha^*}{K_{\alpha=1}^*}, \tag{42}$$

$$\chi_\mu = \frac{\mu_\alpha^*}{\mu_{\alpha=1}^*}, \tag{43}$$

$$\chi_E = \frac{E_\alpha^*}{E_{\alpha=1}^*}, \tag{44}$$

$$\alpha = \frac{1}{N}\sum_{i=1}^{N}\frac{a_i}{b_i}, \tag{45}$$

where $K_{\alpha=1}^*$, $\mu_{\alpha=1}^*$ and $E_{\alpha=1}^*$ (K_α^*, μ_α^* and E_α^*) are, respectively, the predicted effective bulk modulus, the effective shear modulus and Young's modulus, when $\alpha = 1$ ($\alpha < 1$). The effective properties $K_{\alpha=1}^*$, $\mu_{\alpha=1}^*$, $E_{\alpha=1}^*$, K_α^*, μ_α^* and E_α^* can be obtained using the iteration schemes. See details in [15].

It is noted that Eqs. (37)–(43) in our latest work [15] are derived based on the assumption that the properties of deposition products and intrinsic concrete are identical for each other. However, the properties of intrinsic concrete are usually not equal to those of the deposition products. The homogenization process should be performed before these equations are adopted. It implies that K_2 and μ_2 in Eqs. (37)–(43) of [15] (i.e., the bulk modulus and shear modulus of the deposition product in Eqs. (37)–(43) of [15]) should be replaced by K_{av} and μ_{av}, which are obtained by the following expressions:

$$K_{\text{av}} = 0.5\left[\phi_G K_{\text{dp}} + (1-\phi_G)K_{\text{em}}\right] + 0.5\left[\frac{K_{\text{dp}}K_{\text{em}}}{\phi_G K_{\text{em}} + (1-\phi_G)K_{\text{dp}}}\right], \tag{46}$$

$$\mu_{\text{av}} = 0.5\left[\phi_G \mu_{\text{dp}} + (1-\phi_G)\mu_{\text{em}}\right] + 0.5\left[\frac{\mu_{\text{dp}}\mu_{\text{em}}}{\phi_G \mu_{\text{em}} + (1-\phi_G)\mu_{\text{dp}}}\right], \tag{47}$$

$$\phi_G = \frac{V_{\text{dp}}}{V_{\text{dp}} + V_{\text{em}}} = \frac{(1-\phi_{\text{FD}})\,(S_{\text{eff}}\phi_{\text{eff}})}{1-\phi_{\text{FD}}(S_{\text{eff}}\phi_{\text{eff}})}, \tag{48}$$

where K_{av}, μ_{av} are the effective bulk modulus and shear modulus of the equivalent material made up of the deposition products and the equivalent matrix; ϕ_G is the volume fraction of the deposition product in the equivalent material; and V_{dp} and V_{em} are the volume of deposition products and the equivalent matrix. Meanwhile, the volume fraction of the inclusion (ϕ_k) should be replaced by ϕ_{aver}, which is as follows:

$$\phi_{\text{aver}} = \frac{V_{\text{wa}}}{V_{\text{dp}} + V_{\text{wa}} + V_{\text{em}}} = \phi_{\text{FD}}(S_{\text{eff}}\,\phi_{\text{eff}}), \tag{49}$$

where V_{wa} is the volume of the water phase.

In addition, the effect of water viscosity in pores can enhance the shear modulus, which means that the shear modulus obtained by Eq. (28) and Eq. (39) should multiply the modification function as follows [15,21]:

$$F = 1 + f_1(S_{\text{eff}}\phi)^2 + f_2 S_{\text{eff}}\phi, \tag{50}$$

where f_1 and f_2 are parameters investigated by experiments [22]. If the nondestructive testing methods, such as the ultrasonic waves, are employed to test the effective dynamic properties of concrete repaired by the EDM, the static properties should be modified into dynamic properties according to the relationships between the two types [15,21]. Specifically, the dynamic Young's modulus can be obtained through multiplying the static Young's modulus by a coefficient reached by experiment [15,21].

Table 1 Properties of intrinsic concrete and water [21]

Properties	Bulk modulus (GPa)	Shear modulus (GPa)
Intrinsic concrete	27.91	18.45
Deposition product	18.61	12.3
Water	2.25	0

4 Verification

4.1 Comparison with experiments and existing models of the EDM

Our predictions are compared with the experimental data and the estimations of the existing models to verify the capacity of the proposed differential-scheme-based micromechanical framework for unsaturated concrete repaired by the EDM.

Firstly, the existing models [21] are utilized to verify our proposed differential-scheme-based micromechanical framework. The predicting results of the different models are compared using four different saturation degrees. The properties of the intrinsic concrete, deposition products and water are listed in Table 1 according to [21].

Figure 4a–c presents the comparison of mechanical properties between predictions in this study and those of [21] during the healing process. From Fig. 4a, it can be observed that predictions herein for the Young's modulus of the equivalent composite are very close to those of [21]. The maximum relative difference between these two predictions is 3 % at the start of the healing when the effective saturation degree is 100 %. With the decrease of the saturation degree, the two predictions are almost identical to each other, which means that the proposed differential-scheme-based micromechanical model is also capable of describing the healing process from the microscale level. Meanwhile, the results of the two different micromechanical models show that the values of effective Young's modulus gradually increase during the healing process due to the accumulation of deposition products. The higher the effective saturation degree is, the greater the equivalent composite becomes during the healing process. As to the effective bulk modulus and shear modulus, predictions in this paper are also similar to those obtained by [21], which are exhibited by Fig. 4b, c, respectively.

Secondly, the Voigt upper bounds and Reuss lower bounds [27,28] are employed to validate the predictive results. The two bounds can be expressed below according to [27,28]

$$\mathbf{D}^R \le \bar{\mathbf{D}} \le \mathbf{D}^V \text{ with } \mathbf{D}^V = \sum_{r=1}^{n} \phi_r \mathbf{D}_r, \quad \mathbf{D}^R = \left[\sum_{r=1}^{n} \phi_r \mathbf{M}_r \right]^{-1}. \tag{51}$$

$\mathbf{D}^V$ and $\mathbf{D}^R$ are the Voigt upper bound and Reuss lower bound stiffness tensors of the composite. $\bar{\mathbf{D}}$ is the effective stiffness tensor of the composite. $\mathbf{D}_r$ and $\mathbf{M}_r$ are the stiffness and compliance tensor of the rth phase. ϕ_r is the volume fraction of the rth phase. It is noted that the bounds are derived in terms of the volume faction of each phase only. Therefore, they are independent of the geometry of the phases and their distribution. For the two-phase composite, the two bounds for the effective bulk modulus and shear modulus can be obtained using the following expression:

$$K^R = \left[\frac{\phi_1}{K_1} + \frac{\phi_2}{K_2} \right]^{-1}, \quad K^V = \phi_1 K_1 + \phi_2 K_2, \tag{52}$$

$$\mu^R = \left[\frac{\phi_1}{\mu_1} + \frac{\phi_2}{\mu_2} \right]^{-1}, \quad \mu^V = \phi_1 \mu_1 + \phi_2 \mu_2. \tag{53}$$

K^V and K^R are the Voigt upper bound and Reuss lower bound for the bulk modulus; μ^V and μ^R are two bounds for the shear modulus. ϕ_1, ϕ_2 (K_1, K_2 and μ_1, μ_2) are the volume fractions (the bulk modulus and shear modulus) of the first and second phase in the two-phase composite, respectively.

Figure 5 presents the comparisons among the results, including the effective shear modulus and the effective Young's modulus, obtained with the proposed micromechanical model, the Voigt upper bounds, the Reuss lower bounds and results of [21] during the healing process. It can be found from Fig. 5 that the predictions of the shear modulus and Young's modulus lie between the upper and lower bounds reasonably. The predictions of [21] are still very near to the results in this study.

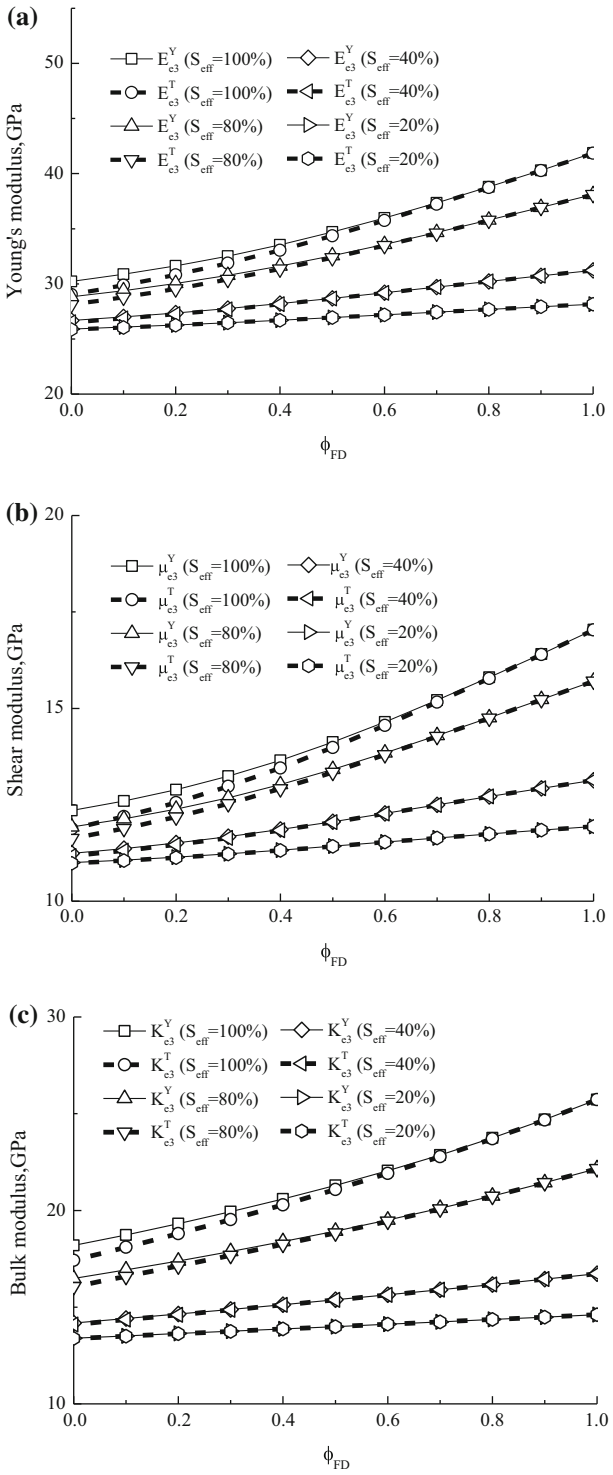

Fig. 4 The comparisons between the predictions of [21] and those in this study at different effective saturation degrees, where E^Y_{e3}, μ^Y_{e3} and K^Y_{e3} represent the predicted effective Young's modulus, shear modulus and bulk modulus of [21]; E^T_{e3}, μ^T_{e3} and K^T_{e3} represent those in this study. **a** The Young's modulus, **b** the shear modulus, **c** the bulk modulus

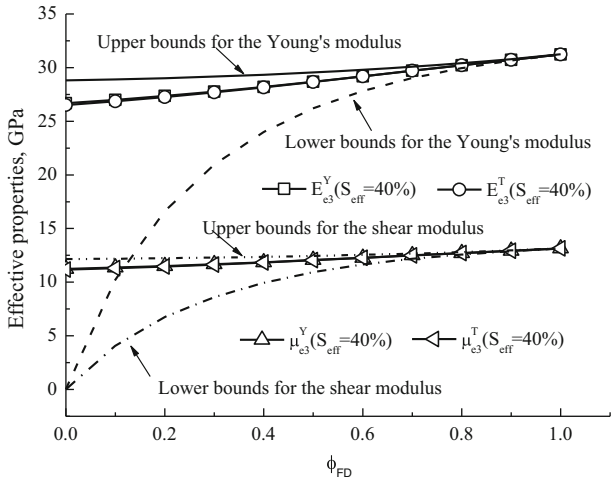

Fig. 5 The comparisons among the predictions of Yan et al. [21], the Voigt upper bounds, Reuss lower bounds and those in this study, where E^{Y}_{e3} and μ^{Y}_{e3} represent the predicted effective Young's modulus and shear modulus of Yan et al. [21]; E^{T}_{e3} and μ^{T}_{e3} represent those in this study

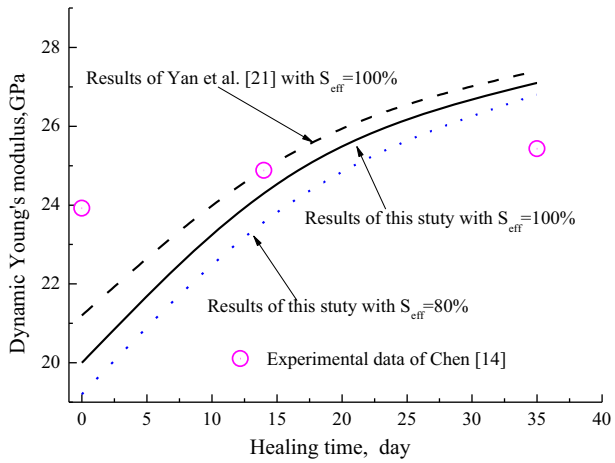

Fig. 6 Comparison among the results of Yan et al. [21], results obtained with the proposed model and those obtained experimentally [14] for the dynamic Young's modulus in the dry state

Thirdly, with the modifications in Sect. 3.4, the differential-scheme-based micromechanical model for the healed unsaturated concrete can be modified to predict the properties of the healed specimen when they are dried. Here, the dynamic Young's moduli in the dry state of the specimen before and after healing in Chen's experiment [14] are adopted to validate the proposed micromechanical model. The average initial porosity of the specimen is 0.299. The average pulse velocity of its intrinsic concrete is 5134.5 m/s. The density is 2537.9 kg/m^{3}and the Poisson ratio is 0.229. As exhibited in Fig. 6, the predictions obtained from the micromechanical model correspond reasonably with those obtained experimentally. Overall, the predictions in this paper are still close to those of Yan et al. [21].

In summary, the comparisons between our predicting results and those obtained experimentally, and those reached by the existing models show that the proposed differential-scheme-based micromechanical model can quantitatively describe the healing process of unsaturated concrete reasonably at the microscale level.

4.2 Comparison with experiments and existing models at two extreme states of the EDM

In this section, our predictions at two extreme states of the EDM are examined to further validate the proposed differential-scheme-based micromechanical framework.

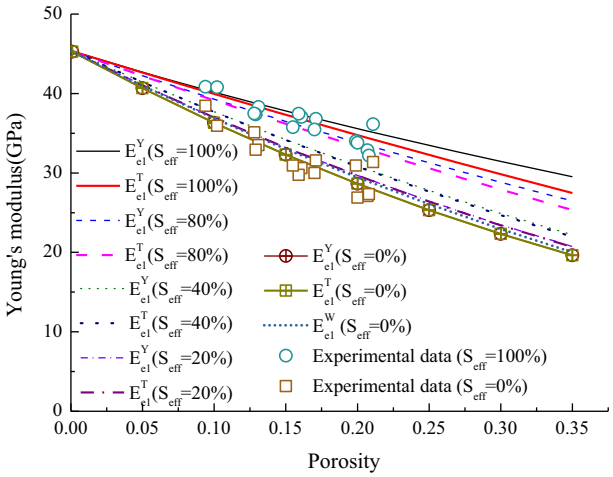

Fig. 7 Comparison among the results of this study, existing models and those obtained experimentally [26] for the Young's modulus of the unsaturated concrete, where E^Y_{e1}, E^W_{e1} and E^T_{e1} represent the predicted effective Young's modulus of Yan et al. [21], Wang and Li [22] and this study for unsaturated concrete

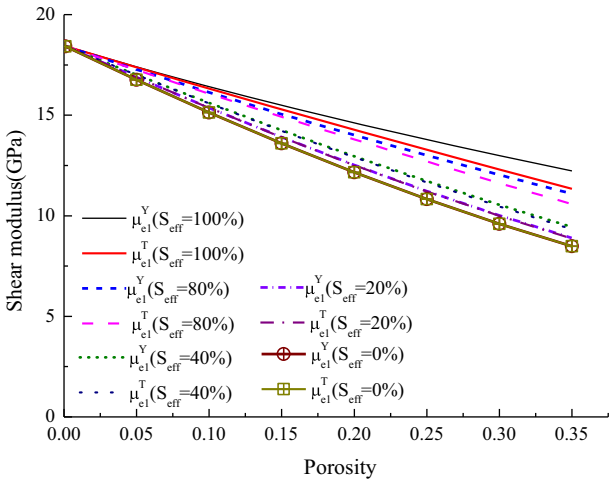

Fig. 8 Comparison between the results of this study and existing models for the shear modulus of the unsaturated concrete, where μ^Y_{e1} and μ^T_{e1} represent the predicted effective shear modulus of Yan et al. [21] and this study for unsaturated concrete

The first extreme state is that there is absolutely no healing process in the concrete. Figure 7 exhibits the comparisons among results in this study, those obtained by [21], those of [22] and the experimental data of [26]. The comparisons show that predictions herein are close to those of existing predictions and agree well with the experimental data. For the dry state ($S_{\text{eff}} = 0$), the estimations in this study are the same as in [21]. As to the effective shear modulus and bulk modulus, the similar conclusions can be reached, which are exhibited in Figs. 8 and 9.

The second extreme state is that the saturated zone has been completely healed by the EDM. Therefore, the healed unsaturated concrete is effectively a three-phase composite with the isotropic spherical inclusion phase and different shapes of pores. The experiment of Cohen and Ishai [51] is adopted to further verify the proposed model. In their work, the porous composite, where both silica particles and porosity coexist, has respective volume fractions varying from 12 to 33.25 and 10 to 30.5 %. According to our proposed micromechanical framework, the effective properties of the porous composite can be calculated. It can be found from Table 2 that estimations herein are very close to the experimental data. The average error in our predictions relative to experimental results is about 8 %. The predictions are always lower than the upper bounds and higher than the lower bounds.

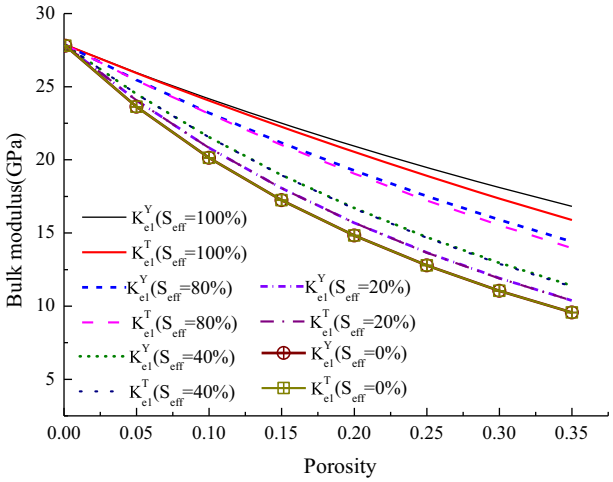

Fig. 9 Comparison between the results of this study and existing models for the bulk modulus of the unsaturated concrete, where K_{e1}^{Y} and K_{e1}^{T} represent the predicted effective bulk modulus of Yan et al. [21] and this study for unsaturated concrete

Table 2 The predicted and experimental elastic moduli of porous composites

Particle volume fraction (%)	Porosity volume fraction (%)	E^*/E_0			
		Experimental [51]	Reuss lower bound	Voigt upper bound	Predicted this paper
15.75	10	1.15	0	6.11	1.22
22.25	25	1.13	0	8.11	1.09
23.25	21.5	1.07	0	8.48	1.18
23.5	20	1.17	0	8.58	1.22
26.75	10	1.73	0	9.75	1.55
27.75	6.5	1.9	0	10.12	1.68
33.25	14	1.48	0	11.86	1.68

Furthermore, if the effective saturation degree is 100 %, the repaired concrete turns to the two-phase composite with the spherical inclusions after complete healing. The works done by Smith [52] are employed to verify this special case at the second extreme state. Figure 10a, b presents the comparisons among our results, those obtained by [21], the upper bounds, the lower bounds and the experimental data of Smith [52]. From Fig. 10a, it can be found that our predictions for the Young's modulus and those of [21] agree well with the experimental data when the volume fraction of the particle is low. These two predictions lie between the upper bounds and lower bounds reasonably. However, predictions herein correspond much better with the experimental data than those of [21] when the volume fraction of the particle increases to 0.4–0.5. Similar conclusion can be reached when the shear modulus is considered according to Fig. 10b.

In summary, our proposed differential-scheme-based micromechanical framework for unsaturated concrete repaired by the EDM can predict the properties of the unsaturated/saturated concrete or the spherical particle reinforced (porous) composite at the extreme states. Compared with the previous models [21], the predictions of this new framework agree well and better with the experimental data when the volume fraction of the inclusion is higher. We also refer to [53].

5 Conclusions

The electrochemical deposition method (EDM) is a newly developed healing method for deteriorated concrete in a water environment. Many meaningful experimental studies have been performed to evaluate its healing effectiveness. However, there are limited theoretical models, especially micromechanical models, available for describing the healing process of the concrete repaired by the EDM at the microscale level. As an extension of our latest work, an equivalent matrix for unsaturated concrete is attained through the micromechanical homogenization to a two-phase composite composed by the intrinsic concrete and unsaturated pores with dif-

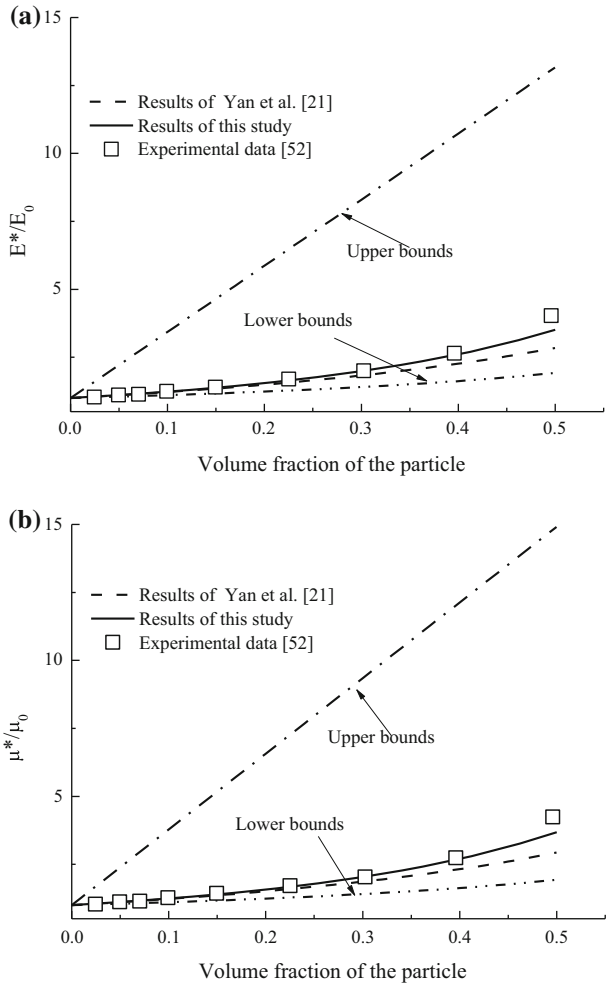

Fig. 10 The comparisons among our results, those obtained by Yan et al. [21], the upper bounds, lower bounds and the experimental data of Smith [52] for the properties of two-phase composite. **a** The Young's modulus, **b** the shear modulus

ferent shapes. It is found that the effective saturation degree and the equivalent aspect ratios of the pores play important roles in determining the properties of the equivalent matrix. The differential-scheme-based micromechanical framework is proposed with the equivalent matrix to quantitatively describe the healing process of unsaturated concrete healed by the EDM. Three different states for the healing process are quantitatively investigated. Furthermore, the predictions are compared with those of the existing micromechanical models and the experimental data. The following conclusions can be reached:

(1) The proposed differential-scheme-based micromechanical models can quantitatively predict the mechanical properties of unsaturated concrete repaired by the EDM during the entire healing process.
(2) As special cases, the micromechanical framework can accurately estimate the effective properties of the saturated concrete repaired by EDM, the unsaturated/saturated concrete and the spherical particle reinforced (porous) composite.
(3) Compared with the results of our latest models, the estimations of this differential-scheme-based micromechanical framework agree well and better with the experimental data when the volume fraction of the inclusion is higher.

Acknowledgements This work is supported by the National Key Basic Research and Development Program (973 Program, No. 2011CB013800) and National Natural Science Foundation of China (51508404, 51478348, 51278360, 51308407). This work is also supported by Key Laboratory of Advanced Civil Engineering Materials (Tongji University), Program of Shanghai Science and Technology Commission(15DZ1205003), the 1000 Talents Plan Short-Term Program by the Organization Department of the Central Committee of the CPC, Research Program of State Key Laboratory for Disaster Reduction in Civil Engineering, the

Scientific Platform Open Funds of Fundamental Research Plan for the Central Universities, Chang'an University (310821151113) and Natural Science Foundation of Shandong Province (ZR2013EEL019). The authors declare that they have no conflict of interest.

References

1. Yokoda, M., Fukute, T.: Rehabilitation and protection of marine concrete structure using electrodeposition method. In: Proceedings of the International RILEM/CSIRO/ACRA Conference on Rehabilitation of Concrete Structures, RILEM, Melbourne, pp. 213–222 (1992)
2. Sasaki, H., Yokoda M.: Repair method of marine reinforced concrete by electro deposition technique. In: Proceedings of the Annual Conference of Japanese Concrete Institute, pp. 849–854 (1992)
3. Jiang, Z.W., Li, W.T., Yuan, Z.C.: Influence of mineral additives and environmental conditions on the self-healing capabilities of cementitious materials. Cem. Concr. Compos. **57**, 116–127 (2015)
4. Otsuki, N., Hisada, M., Ryu, J.S., Banshoya, E.J.: Rehabilitation of concrete cracks by electrodeposition. Concr. Int. **21**, 58–62 (1999)
5. Otsuki, N., Ryu, J.S.: Use of electrodeposition for repair of concrete with shrinkage cracks. J. Mater. Civil Eng. **13**, 136–142 (2001)
6. Ryu, J.S., Otsuki, N.: Crack closure of reinforced concrete by electro deposition technique. Cem. Concr. Res. **32**, 159–264 (2002)
7. Ryu, J.S.: New waterproofing technique for leaking concrete. J. Mater. Sci. Lett. **22**, 1023–1025 (2003)
8. Ryu, J.S.: Influence of crack width, cover depth, water cement ratio and temperature on the formation of electrodeposition on the concrete surface. Mag. Concr. Res. **55**, 35–40 (2003)
9. Ryu, J.S., Otsuki, N.: Experimental study on repair of concrete structural members by electrochemical method. Scr. Mater. **52**, 1123–1127 (2005)
10. Jiang, L.H., Chu, H.Q.: Influence of concrete parameters on electrodeposition effect. Adv. Sci. Technol. Water Resour. **25**, 23–25 (2005)
11. Jiang, Z.W., Xing, F., Sun, Z.P., Wang, P.M.: Healing effectiveness of cracks rehabilitation in reinforced concrete using electrodeposition method. J. Wuhan Univ. Technol. **23**, 917–922 (2008)
12. Chang, J.J., Yeih, W.C., Hsu, H.M., Huang, N.M.: Performance evaluation of using electrochemical deposition as a repair method for reinforced concrete beams. Struct. Longev. **1**, 75–93 (2009)
13. Chu, H.Q., Jiang, L.H.: Correlation analysis between concrete parameters and electrodeposition effect based on grey theory. J. Wuhan Univ. Technol. **31**, 22–26 (2009)
14. Chen, Q.: The stochastic micromechanical models of the multiphase materials and their applications for the concrete repaired by electrochemical deposition method. Ph.D. dissertation Tongji University, Shanghai (2014)
15. Zhu, H.H., Chen, Q., Yan, Z.G., Ju, J.W., Zhou, S.: Micromechanical model for saturated concrete repaired by electrochemical deposition method. Mater. Struct. **47**, 1067–1082 (2014)
16. Persson, B.: Moisture in concrete subjected to different kinds of curing. Mater. Struct. **30**, 533–544 (1997)
17. Chatterji, S.: An explanation for the unsaturated state of water stored concrete. Cem. Concr. Compos. **26**, 75–79 (2004)
18. Jiang, Z.W., Li, W.T., Deng, Z.L., Yan, Z.G.: Experimental investigation of the factors affecting accuracy and resolution of the pore structure of cement-based materials by thermoporometry. J. Zhejiang Univ. Sci. **14**, 720–730 (2013)
19. Jiang, Z.W., Sun, Z.P., Wang, P.M.: Internal relative humidity distribution in cement paste due to moisture diffusion and self-desiccation. Cem. Concr. Res. **36**, 320–325 (2006)
20. Jiang, Z.W., Sun, Z.P., Wang, P.M.: Autogenous relative humidity change and autogenous shrinkage of high-performance cement pastes. Cem. Concr. Res. **35**, 1539–1545 (2005)
21. Yan, Z.G., Chen, Q., Zhu, H.H., Ju, J.W., Zhou, S., Jiang, Z.W.: A multiphase micromechanical model for unsaturated concrete repaired by electrochemical deposition method. Int. J. Solids Struct. **50**, 3875–3885 (2013)
22. Wang, H.L., Li, Q.B.: Prediction of elastic modulus and Poisson's ratio for unsaturated concrete. Int. J. Solids Struct. **44**, 1370–1379 (2007)
23. Chen, Q., Zhu, H.H., Yan, Z.G., Deng, T., Zhou, S.: Micro-scale description of the saturated concrete repaired by electrochemical deposition method based on Mori-Tanaka method. J. Build Struct. **36**, 98–103 (2015)
24. Chen, Q., Zhu, H.H., Yan, Z.G., Ju, J.W., Deng, T., Zhou, S.: Micro-scale description of the saturated concrete repaired by electrochemical deposition method based on self-consistent method. Chin. J. Theor. Appl. Mech. **47**, 367–371 (2015)
25. Berryman, J.G.: Long-wave propagation in composite elastic media II. Ellipsoidal inclusion. J. Acoust. Soc. Am. **68**, 1820–1831 (1980)
26. Yaman, I.O., Hearn, N., Aktan, H.M.: Active and non-active porosity in concrete part I: experimental evidence. Mater Struct. **35**(3), 102–109 (2002)
27. Qu, J., Cherkaoui, M.: Fundamentals of Micromechanics of Solids. Wiley, Hoboken (2006)
28. Mura, T.: Micromechanics of defects in solids. Kluwer Academic Pub, Dordrecht (1987)
29. Ju, J., Chen, T.M.: Micromechanics and effective moduli of elastic composites containing randomly dispersed ellipsoidal inhomogeneities. Acta Mech. **103**, 103–121 (1994)
30. Ju, J., Chen, T.: Effective elastic moduli of two-phase composites containing randomly dispersed spherical inhomogeneities. Acta Mech. **103**, 123–144 (1994)
31. Weng, G.: Some elastic properties of reinforced solids, with special reference to isotropic ones containing spherical inclusions. Int. J. Eng. Sci. **22**, 845–856 (1984)
32. Weng, G.: The theoretical connection between Mori–Tanaka's theory and the Hashin–Shtrikman–Walpole bounds. Int. J. Eng. Sci. **28**, 1111–1120 (1990)
33. Norris, A.N.: A differential scheme for the effective modulus of composites. Mech. Mat. **4**, 1–16 (1985)
34. McLaughlin, R.: A study of the differential scheme for composite materials. Int. J. Eng. Sci. **15**, 237–244 (1977)

35. Li, G.Q., Zhao, Y., Pang, S.S.: Four-phase sphere modeling of effective bulk modulus of concrete. Cem. Concr. Res. **29**, 839–845 (1999)
36. Nguyen, N.B., Giraud, A., Grgic, D.: A composite sphere assemblage model for porous oolitic rocks. Int. J. Rock Mech. Min. **48**, 909–921 (2011)
37. Ju, J., Zhang, X.: Micromechanics and effective transverse elastic moduli of composites with randomly located aligned circular fibers. Int. J. Solids Struct. **35**, 941–960 (1998)
38. Ju, J., Sun, L.: A novel formulation for the exterior-point Eshelby's tensor of an ellipsoidal inclusion. J. Appl. Mech. **66**, 570–574 (1999)
39. Ju, J., Sun, L.: Effective elastoplastic behavior of metal matrix composites containing randomly located aligned spheroidal inhomogeneities. Part I: micromechanics-based formulation. Int. J. Solids Struct. **38**, 183–201 (2001)
40. Ju, J., Yanase, K.: Micromechanics and effective elastic moduli of particle-reinforced composites with near-field particle interactions. Acta Mech. **215**, 135–153 (2010)
41. Ju, J., Yanase, K.: Micromechanical effective elastic moduli of continuous fiber-reinforced composites with near-field fiber interactions. Acta Mech. **216**, 87–103 (2011)
42. Sun, L., Ju, J.: Effective elastoplastic behavior of metal matrix composites containing randomly located aligned spheroidal inhomogeneities. Part II: applications. Int. J. Solids Struct. **38**, 203–225 (2001)
43. Sun, L., Ju, J.: Elastoplastic modeling of metal matrix composites containing randomly located and oriented spheroidal particles. J. Appl. mech. **71**, 774–785 (2004)
44. Yanase, K., Ju, J.W.: Effective elastic moduli of spherical particle reinforced composites containing imperfect interfaces. Int. J. Damage Mech. **21**, 97–127 (2012)
45. Zhu, H.H., Chen, Q., Ju, J.W., Yan, Z.G., Guo, F., Wang, Y.Q., Jiang, Z.W., Zhou, S., Wu, B.: Maximum entropy based stochastic micromechanical model for two-phase composite considering the inter-particle interaction effect. Acta Mech. **226**, 3069–3084 (2015)
46. Chen, Q., Zhu, H.H., Ju, J.W., Guo, F., Wang, L.B., Yan, Z.G., Deng, T., Zhou, S.: A stochastic micromechanical model for multiphase composite containing spherical inhomogeneities. Acta Mech. **226**, 1861–1880 (2015)
47. Mousavi Nezhad, M., Zhu, H.H., Ju, J.W., Chen, Q.: A simplified multiscale damage model for the transversely isotropic shale rocks under tensile loading. Int. J. Damage Mech. **25**(5), 705–726 (2016)
48. Chen, Q., Mousavi Nezhad, M., Fisher, Q., Zhu, H.H.: Multi-scale approach for modeling the transversely isotropic elastic properties of shale considering multi-inclusions and interfacial transition zone. Int. J. Rock Mech. Min. **84**, 95–104 (2016)
49. Hashin, Z.: The elastic moduli of heterogeneous materials. J. Appl. Mech. **29**, 143–150 (1962)
50. Christensen, R.M., Lo, K.H.: Solutions for effective shear properties in three phase sphere and cylinder models. J. Mech. Phys. Solids **27**, 315–330 (1979)
51. Cohen, L., Ishai, O.: The elastic properties of three-phase composites. J. Compos. Mater. **1**, 390–403 (1967)
52. Smith, J.C.: Experimental values for the elastic constants of a particulate-filled glassy polymer. J. Res. NBS **80A**, 45–49 (1976)
53. Zhu, H.H., Zhou, S., Yan, Z.G., Ju, J.W., Chen, Q.: A two-dimensional micromechanical damage-healing model on microcrack-induced damage for microcapsule-enabled self-healing cementitious composites under tensile loading. Int. J. Damage Mech. **24**, 95–115 (2015)